Communications in Information and Systems
Volume 17, Number 3, 147–169, 2017

SPH-based simulation of liquid wetting across textile materials

Aihua Mao[†], Mingle Wang, Yong-jin Liu[‡],
Huamin Wang, and Guiqing Li

This paper presents a simulation framework for liquid wetting across porous textiles with anisotropic inner structure. The textile is composed by intersected fibers and forms capillary pores in the void space, which provides an important force to drive the diffusion by capillary action. The influence of the properties of the textile on the wetting process, such as contact angle, hygroscopicity and porosity, is considered into the liquid wetting process in detail. By liquid-textile coupling, the wetting process is simulated through liquid absorption/desorption by fiber and liquid diffusion in the means of inner fiber, intersected fibers and capillary action. The second Fick's law is used to describe the non-steady wetting process. Based on the SPH method for fluid simulation, this framework can simulate the liquid wetting across the porous textile by dripping single or multiple drops of water. We also demonstrate the wetting process with the influence of different properties of the textile.

1. Introduction

Physically-based fluid simulation is one of the hot research topics in computer graphics, which has a wide range of applications in virtual reality, digital entertainment and scientific visualization. The related works have been widely conducted with the focus on the mere fluid [9],[7],[18], or the mixed fluid with other mediums, such as fluid-rigid [6] and fluid-deformable[12].

[†]Research supported by NSF of Guangdong Province under Grant 2016A03 0313499, The Science and Technology Planning Project of Guangdong Province under Grant 2015A030401030 and the Fundamental Research Funds for the Central Universities under Grant2017ZD054.

[‡]Research supported by the Natural Science Foundation of China (61725204, 61661130156) and Beijing Higher Institution Engineering Research Center of Visual Media Intelligent Processing and Security.

The research on mere fluid simulation have already reproduced either huge-scale fluid [17] (tornado, ocean waves, and water fall) or small-scale fluid detail to water drops [24]. The research on mixed fluid with rigid (solid) [26] or deformable (liquid, gas) [11] involves more complex micro-interactions and receives more attentions in recent days. In this filed, most of the work concentrates on the mixture of fluid with other mediums on particle-particle level without consideration of the liquid absorption and diffusion phenomena. However, in practice many solid materials are penetrable and with porous structure, which allows liquid absorption and diffusion across the material. That is an important physical property determining the moisture management functions of the materials and is a key issue for material manufactures and consumers. For instance, the fabric materials are usually evaluated by the fast-drying and sweat-absorption abilities for clothing design. To extend the research scope to porous material, Toon et. al [15] and Saket et. al [21] carried out the research of fluid simulation for porous flow and porous solid respectively. Later, Shi et. al [22] integrated Saket et. al's work [21] with wetting clothing research [15][13] for simulating fluid absorption and diffusion for porous material. However, Toon et al. [15] consist of the porous materials by particles which just work for isotropic diffusion without structure influence in the materials. Saket et. al [21] and Shi et. al [22] regarded the porous cloth as geometric surfaces represented by meshes and without structure on the thickness, which is a common treatment in wetting clothing research. Though they claimed to model anisotropic diffusion by setting different values of a weight coefficient for different surface triangles, it can not really realize the anisotropic diffusion caused by the material's internal structure. All the current works are based on simply representing the porous material with meshes or particles. In fact, the inner structure of porous materials greatly influences the involved physical behaviors, such as liquid absorption and diffusion, and can not be ignored in the physical-based simulation. To fill in this gap, we push on the research to the anisotropic fluid simulation of porous materials considering the realistic inner structure.

In this paper, we propose a new simulation framework for liquid wetting across the porous textiles based on Smoothed Particle Hydrodynamics (SPH) method. The porous textiles are constructed by intersected fibers and have porous inner structure, which leads to anisotropic fluid flow across it. As a mixture of fluid-rigid, we develop a SPH-based method to simulate the liquid wetting including absorption and diffusion across the porous textile structure. To achieve more realistic simulation, we concern both liquid absorption and desorption during liquid wetting, which is more loyal to the fiber moisture behavior in practice, and model the influence of the properties

of textile, such as contact angle, hygroscopicity and porosity in the wetting process.

The main contributions of our work are as follows:

1. We propose a new physically-based simulation of liquid wetting across porous textiles, which is the first work in our knowledge to establish a framework of fluid simulation for porous materials with real anisotropic inner structure.

2. Liquid absorption and desorption during fluid diffusion is concerned as a dynamic balance process according to the physical investigation in literature, which offers a consistent basis to simulate practical fiber moisture behavior.

3. By considering the contact angle of material surface in determining the amount of liquid absorption, this simulation framework can truly manifest the hydrophilic/hydrophobic property of the textile, while previous works on porous fluid simulation rarely take the surface attribute into account.

4. By utilizing the second Fick's Law, the non-steady liquid wetting across the porous textile is simulated in terms of liquid aborption/desorption by the fiber and liquid diffusion by the means of inner fiber, intersected fibers and capillary action, which can achieve more realistic simulation of the anisotropic and nonlinear liquid wetting process.

2. Framework overview

The framework of simulating liquid wetting across the porous textile contains three modules (shown in Fig.1). As a SPH-based simulation method, we first carry out the fluid simulation based on SPH framework. However, different from the traditional one, except for the density, pressure, viscosity, we deliberately investigate and calculate the surface tension and consider the influence of contact angle on the liquid wetting of textile through interfacial tension equilibrium. Meanwhile we build up dynamic grids for particle neighborhood search to reduce the computation cost. The second the module is porous textiles construction, which does not regards the textile as particles or non-structure surface representation, while adopt a multi-level construction method to represent the realistic anisotropic structure of the porous textiles. By this method, the textile is constructed by intersected fibers, which is divided into fiber segments for detail simulation and visualization of the liquid content distribution of the fiber. Further, the fiber segment is modeled by triangle meshes to conduct the liquid-solid interaction. For better performance of collision diction, hierarchical boundary boxes are developed for the fiber segment, fiber, and textile respectively.

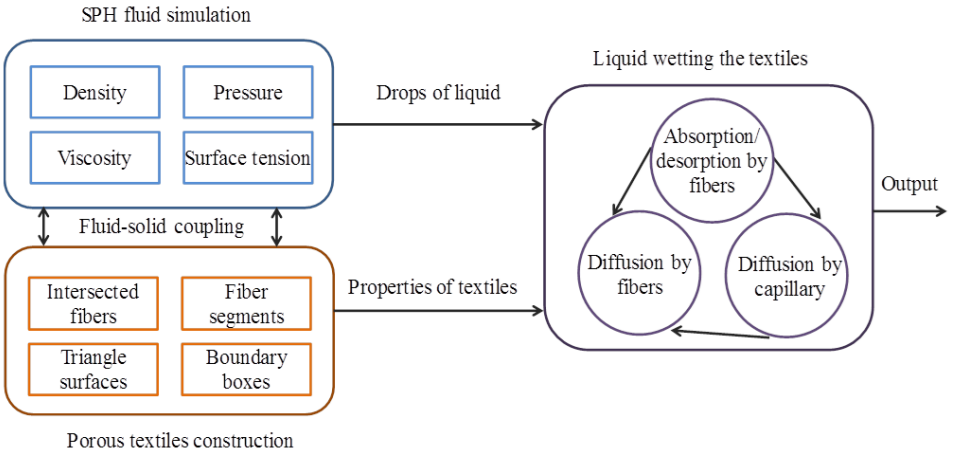

Figure 1: An overview of different steps in our framework.

Provided with the representation of fluid and porous textile, we realize the simulation of liquid wetting across the textile based on fluid-solid coupling, which is achieved by collision detection between particles and surface meshes of the fiber segments. Then we simulate the wetting process in detail in terms of liquid absorption/desorption by fibers, liquid diffusion by fibers and liquid diffusion by capillary force. In these physical behaviors, the properties of the porous textiles, such as the contact angle, hygroscopicity and porosity are considered into the modeling of wetting process in the microscope view. Considering that the liquid diffusion across the textile is a non-steady process, we adopt the second Fick law to describe it and realize anisotropic diffusion in the means of inner fibers, intersected fibers and capillary action. Our simulation framework is based on the consideration of real inner structure of the porous textile results and can achieve realistic simulation results.

3. SPH fluid flow

3.1. Fluid simulation

The particle-based simulation directly quantifies the volume fraction of liquid absorption/desorption and diffusion during wetting and wicking. The density, pressure and viscosity of the fluid can be calculated by the traditional SPH method, which can be referred to the literature [20]. In order to

simulate the influence of the surface characteristic of the textile in liquid wetting, we concern the contact angle of fluid on the interface with other medium such as fibers in the surface tension to reflect the hydrophilic/hydrophobic property of the textile materials, which lays the foundation for achieving more realistic simulation results.

Surface tension is the cohesive force exerted upon the surface molecules of a liquid to be pushed together and have the least surface area. It appears on the interface of two different phases, such as liquid-air and liquid-solid, resulting in different densities and interactions between the molecule. In the SPH framework, the interaction force of the molecule is treated as the interaction force of the particles. The surface tension force is exerted on the particles near the fluid surface, and can be calculated based on the work of Morri [19] and Muller [20] as follows:

$$\vec{F}_{surfaceTension} = \delta\kappa\hat{n} \tag{1}$$

where δ is the surface tension coefficient, κ is the curvature of the liquid surface and $\hat{n}$ is the gradient direction near the surface. Thus the surface tension force is measured by the scalar density (C_s) :

$$\vec{F}_{surfacetension} = \sigma\kappa\frac{-\nabla^2 C_s}{|\nabla C_s|} = \sigma\nabla^2 C_s \nabla C_s/|\nabla C_s| \tag{2}$$

In our work, wetting of textile fibers is the displacement of a fiber (solid)-vapor interface with a fiber (solid)-liquid interface. The boundary of the solid-liquid interface is the balance result of solid-vapor, liquid-vapor, and solid-liquid tension, in which liquid-vapor tension refers to the surface tension of the fluid above. In this balance system, the term equilibrium contact angle is defined based on the interfacial tension equilibrium in the Young-Dupre Equation:

$$\cos\theta = \frac{\gamma_{SV} - \gamma_{SL}}{\gamma_{LV}} \tag{3}$$

where $\gamma_{SV}, \gamma_{SL}, \gamma_{LV}$ are the surface tensions at the solid-vapor, solid-liquid and liquid-vapor interfaces.Wettability increases with the decrease in the equilibrium contact angle. When the contact angle is close to 0°, the material is good at liquid absorption (hydrophilic). When the contact angle approaches 90°, the material rejects liquid absorption (hydrophobic).

In practice, at the contact moment the contact angle between the liquid-vapor interface and liquid-solid interface is not equal to the contact angle in the balance state. The dynamic change of contact angle is difficult to

describe in the simulation. Thus, we concern this change in another way, namely changing of the height of liquid drop. In this way, we change the pressure at the bottom of the fluid to change the area of the liquid-solid interface then to reach balance again, which is approximated by lifting or reducing the height in the capillary tube:

$$h = 2 * F_{surfacetension} \cos\theta / \rho g r \tag{4}$$

where h is the lift or reduced height in the capillary tube, θ is the contact angle, and ρ is the density of the fluid, g is the gravity and r is the radius of the capillary.

3.2. Dynamic space grids

As a Lagrangian method, the SPH model with more particles will lead to more realistic simulation results. However, the large among of particles is a great burden on calculation, which means it's difficult to realize real-time simulation. In the calculation load, an important part comes from the searching of neighbor particles, which determine the interpolation for the attributes of a particle. The searching task repeats during the calculation of density, pressure, viscosity and surface tension for each frame. Thus an intuitive treatment is to mark all the particles in the space before the calculation, and the particles outside the range of smooth kernel radius will be excluded, which helps to greatly reduce calculation load.

In order to efficiently mark the particles, we employ space grids whose boundary can be easily determined according to the boundary of the fluid. The smooth kernel radius which means the influence radius is used as the grid step to divide the grids. Every particle in the fluid has its own space coordinate. According to the coordinate of a particle in fluid, the grid index of the particle on the x,y,z axis can be obtained by the grid step which is the mark for the particles. After setting the particles into the grids, it will be convenient when the calculation happens. The search range of neighborhood for a given particle includes the grid holds the particle and its neighboring grids (as shown in Fig.2).

However, due to the irregular shape of the fluid, the space grids will waste lots of space which does not fully cover the fluid. Even in the case that the volume of the fluid is large while the smooth kernel radius is small, the number of grids will take too much memory resource. Thus, here we solve this problem by dynamic creation of the space grids.

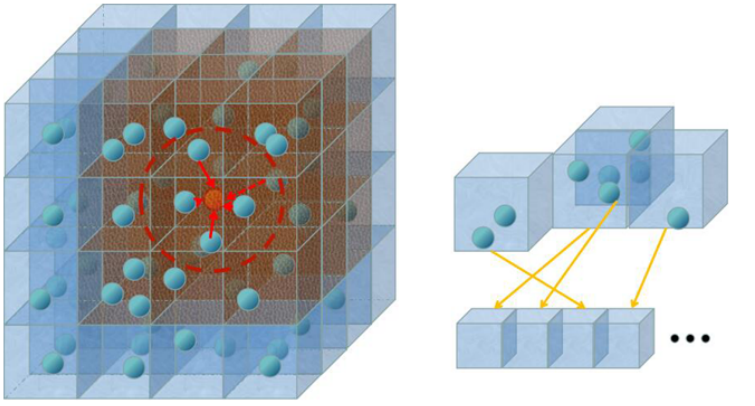

Figure 2: Dynamic space grid for marking the particles, left is neighboring particles searching,right dynamic grid creation.

After calculating the grid index for a given particle, if the space grid holding this particle does not exist, we create the grid and add it to the grid sequence (shown in Fig.2), meanwhile, build up a mapping between the grid index and the sequence index so that this grid can be quickly found. By this way, we can avoid wasting empty grids and improve the utilization of the memory resource during computation.

4. Construction of porous textiles

In computer graphics, simulation of porous textiles such as fabric and clothing is a continuous research interest. Early simulation methods used particle systems [5][10], which is a simple and intuitive modeling way and is flexible in conjunction with other numerical schemes. More popular modeling methods are based on mass-spring grids to simulate the elasticity and deformation of materials, such as David E. Breen's [4], Wang [24], Cirio [8]. They can provide real-time simulation and offer interactive tools while are deficient in modeling surface elasticity accurately [25] . Also the mass-spring methods are inaccurate for anisotropic and nonlinear models [2]. Recent work has applied Lagrangian finite element for simulating anisotropic and nonlinear cloth materials under large deformations [23]. Though the finite element methods are more accurate to model deformable volumetric solids [3], it tends to result in impractically high computation cost, which usually needs appropriate simplifications for interactive graphics applications.

In the simulation of the fluid on cloth or flow through the porous solid, modeling the cloth or textiles is based on different methods in literature. Lenaerts et al. [15] adopted the particle-based modeling of solid to represent small porous volume for holding an amount of fluid, Patkar [21] and Huber [13] used finite element-based method which continuously models the solid with meshes, thus can not explicitly consider the effect of pore on fluid flow. As mentioned in Section 1, these modeling methods can not reveal the real porous structure of the solid, which leads to non-realistic simulation of fluid flow through the porous solid, such as the anisotropic diffusion across the textile can not be realistically simulated.

Based on the idea from [27], we construct the porous textiles by yarn models to represent the realistic material structure. The textile is composed by weft and warp fibers, and the fibers are modeled under a 1D curvature to be intersected on the weft and warp directions. For the purpose of visualization of the fiber liquid content, we further divide the fiber into a set of segments by the unit of a half of loop, and represent the fiber segments by triangle meshes. When the weft and warp fibers are combined by interval interaction, the porous textile is constructed. The fiber-level details determine the structure of textile, such as, the porosity of the textile, which means the volume fraction of interconnected void space to the total textile volume, and is also reflected by the density property. As shown in Fig.3 the fibers with different diameters lead to different porosity of textiles. In physics, porosity of the solid is an important property exerting a pressure on the fluid, which greatly influences the fluid diffusion in the porous material. In order to naturally concern it in the simulation, given a textile with square size and consisted by a single fiber, it can be calculated by:

$$\varepsilon_{textile} = 1 - \sum_{i=0}^{n} \pi r_{fiber}^2 \cdot l_{fiber} / \left(2r_{fiber} \cdot (l'_{fiber})^2\right) \tag{5}$$

where $\varepsilon_{textile}$is the porosity of textile, $r_{fiber}$is the radius of fiber, n is the number of fibers, $l_{fiber}$is the origin length of fiber, and $l'_{fiber}$is the bended length of fiber which can be obtained with the given curvature of fiber.

The fiber segments play the role of basic geometric units for undertaking physical behaviors. During the liquid wetting process, the fluid is diffused from the location with high concentration to surrounding area with low concentration. The liquid content of a fiber is not uniform at different locations. In practice, it significantly distributes along the length direction. We divide the fiber into a number of segments, which is divided by the unit of half of a loop. The concern is that half of a loop segment is convenient to construct

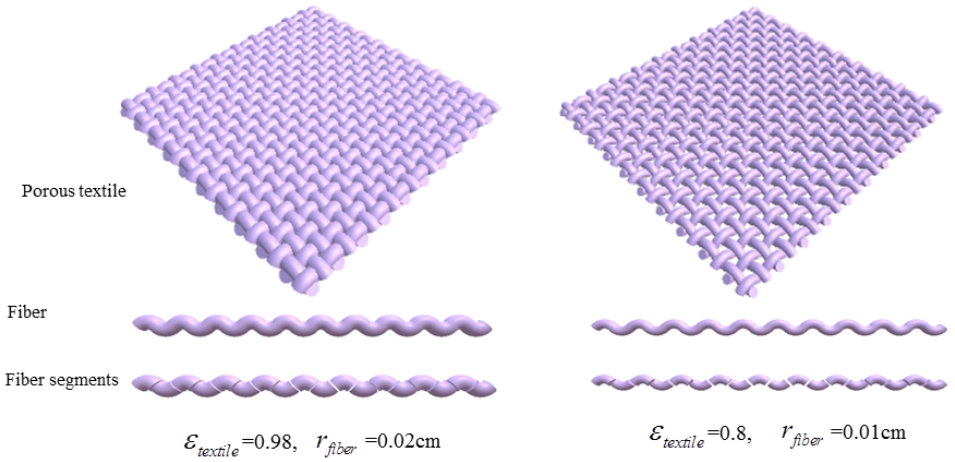

Figure 3: The textile with different porosities when constructed by fibers with different diameters.

intersected fibers, and meanwhile is enough to distinguish the concentration gradient of liquid content in the fiber. During the liquid absorption and diffusion, a segment of the fiber is regarded as the smallest unit to consider the wetting process, which provides a fine-grained level of simulation of the liquid wetting across the textiles.

By the geometric representation, the fiber segment is modeled by thousands of triangle meshes, which is regarded for the objects which will have interactions with the fluid, such as collision. However, the great amount of triangle meshes will lead to heavy computation for every particle-every triangle mesh collision detection. Concerning this problem, we develop bounding boxes for the textiles in hierarchal layers corresponding to its multi-level construction. Concerning the textile constructed by weft and warp fibers regularly, AABB bounding box is used for speeding up the collision detection. As shown in Fig.4, the boundary boxes for a textile and composed fibers and fiber segments are developed hierarchically level by level. As to the geometric relationship, the boundary vertices of higher level bounding box are just obtained from the maximum and minimum vertices of all bounding boxes in the lower level, which reduce the computation cost in updating boundary vertex of the bounding boxes. In this method, the hierarchal bounding boxes are efficient to reduce the times of collision detection through level by level filtering. Such as, particles which have collision with the bounding box of the textile, then continue to be detected with the bounding box of the fiber, and similarly, the particles which have collision with the bounding

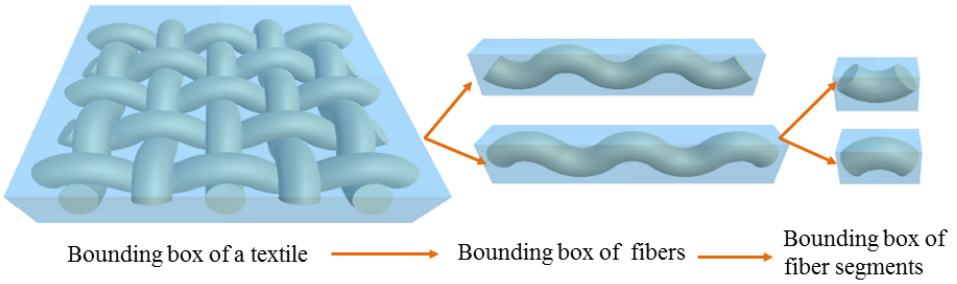

Figure 4: Hierarchal bounding boxes according to the multi-layer textile model.

box of the fiber, then continue to be detected with the bounding box of the fiber segment, lastly, the particles which have collision with all the bounding boxes of the textiles, a fiber and a fiber segment will be detected with the triangle meshes on the collided fiber segment.

It is noted that in practice many real yarns have very complex structure, which leads to great difficulty to determine the size of the pore and can not exactly simulate the capillary diffusion. Meanwhile, the more number of twisted fiber even with various length in the yarn structure, the more difficulty to simulate the diffusion between inter-fibers. Thus, all the current related papers did not concern the real yarn structure in the fluid simulation. Furthermore, on the yarn level, it is too complex to consider the liquid absorption/desorption by single fiber, and also the diffusion between fibers/yarns in the view of meshes. Thus it is better to choose single fiber to weave textile to actualize the simulation framework.

5. Liquid wetting across porous textiles

The flow of liquid across the textiles is caused by fiber-liquid molecular attraction at the fiber surface, which is driven by surface tension and capillary force. We firstly realize the liquid-textile coupling in the view of particle collision detection, and then simulate the wetting process by considering the liquid absorption/desorption by the fiber and liquid diffusion cross the textile. Concerning the anisotropic structure of the textile, the liquid diffusion occurs in terms of diffusion by inner fiber, intersected fibers and capillary action respectively.

5.1. Liquid-textile coupling

The liquid and textile are coupled when the liquid come to contact with the textile surface. Since the liquid is expressed by particles and the textile is represented by the unit of the triangle meshes of fiber segments, the liquid-textile coupling is considered by the interaction between the liquid particles and fiber segment meshes, which is realized by collision detection in the simulation.

The basic collision detection between a particle and a triangle mesh is performed by two steps, namely, firstly computing the distance of the particle to the mesh surface and checking whether the distance is within a given threshold of collision, then further projecting the particle onto the mesh surface and checking whether the projection point is within the area of the surface. If the distance is greater than the threshold or the projection point is outside of the surface, the collision is not detected. Besides of the conditions in these two steps, some issues still need to be concerned.

One is the motion direction of the particle. If the motion direction of the particle is away from the triangle surface, there is no possibility of collision. Since the normal vector of the triangle surface is outward, when the angle between motion direction of the particle and the normal vector is smaller than 90 degree, it denotes the particle is moving away from the triangle surfaces. In such case, the collision will never happen. If that angle is great than 90 degree, it denotes the particle is moving forward to the triangle surface and the collision detection is possible to happen. If the angle is just 90 degree, the particle just moves parallel with the triangle surface and maybe stop on the surface due to friction or move away from the surface. When the particle stops on the surface, we regard that the collision is detected. Fig.5 demonstrates these three cases of different angle values. For computation efficiency, this issue is dealt with before the basic collision detection.

Another is the velocity of the particles, which may be too fast to be detected. Occasionally, the velocity is fast enough for a particle to penetrate through the fiber within the time step of a single frame, which will cause the mistake of collision judgment. Though this issue may be solved by reducing the time step, it leads to great cost of heavy computation. We use an idea of pre-detection to avoid this situation. After the collision detection in the current frame, we predict the position of the particle in the next frame so that we can find out whether the particle will penetrate through the fiber. If this happens, we mark down that the particle will have collision in the next frame.

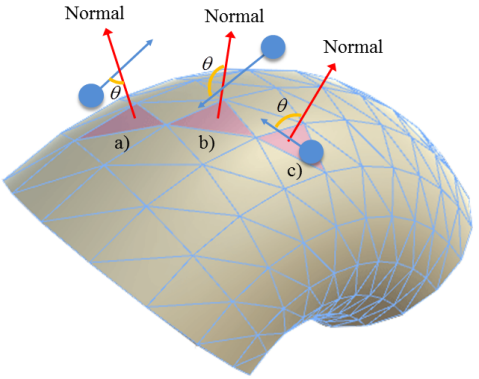

Figure 5: The angle between motion direction of the particle and the normal vector expresses three cases: a) small than 90 degree, no collision; b) great than 90 degree, possible collision; c) equal 90 degree, collision or move away.

Once the particle has collision with the fiber segment, we further deal with it by concerning the physic behavior of liquid absorption. That is, if the fiber segment is not saturated, the particle will be absorbed by this fiber segment and is regarded as in the dead status. Otherwise, the particle will be bounced off the mesh surface of the fiber segment. Since the mass ratio between a particle and a textile is very slight, the momentum of the motion during the collision is approximately conserved and the particle is bounced off in the specular direction with the same velocity norm.

5.2. Liquid absorption/desorption

When the fiber is placed in an environment at certain temperature and relative humidity, it can hold amount of moisture. The moisture exchange between fiber and air is kept happening in term of sorption/desorption processes, which finally reaches equilibrium water content in the fiber. In the physic investigation, the process of liquid absorption/desorption by the fiber is a dynamical process, while is related to surrounding air relative humidity, the liquid concentration of the fibers and also its surface property [16]. Fiber hygroscopicity is generally used to define the ability to absorb moisture. High hygroscopicity and water content in the fiber usually leads to liquid desorption if the fiber is saturated. In order to quantify the liquid volume absorbed/desorbed in the liquid wetting, here we adopt the fiber moisture balance equation proposed by Li and Zhu [16], which expresses that the liquid content of the fiber in the unit area and time is the dynamic

equilibrium result of the absorption rate and desorption rate:

$$\frac{\partial C_f}{\partial t} \propto constant \cdot \rho \cdot W_{cs}(RH) \cdot (D_f / R_f^2) \tag{6}$$

where $C_f$is the liquid content of fiber, $\rho$is the fiber density, W_{cs} is the liquid content at the fiber surface determined by the sounding air relative humidity (RH), R_f is the fiber's radius, D_f is the liquid diffusion coefficient of the fiber, here we use kunzel's diffusion coefficient [14] to determined D_f:

$$D(c_l) = 3.8 \cdot \left(\frac{A_w}{\rho_l \cdot c_s} \right) \cdot 1000^{-\frac{c_l}{c_s}} \tag{7}$$

where A_w is the liquid absorption coefficient, $\rho_l$is the density of the water,$c_s$is the saturation liquid volume , and $c_l$is the current liquid concentration difference.

With the result of $\frac{\partial C_f}{\partial t}$, we can further calculate the liquid absorption/desorption rate of the contact area on the fluid-solid interface by $S_{contact}\frac{\partial C_f}{\partial t}$. $S_{contact}$is the contact area, which can be calculated by the interface energy and the contact angle:

$$S_{contact} = \frac{S_{geometric} E_{lv} \cos\theta}{E_{sv} - E_{sl}} \tag{8}$$

where $S_{geometric}$ is the theoretical contact area on the smooth surface, E_{lv}, E_{sv}, E_{sl} are the surface energy of the liquid-vapor interface, the solid-vapor interface, and the solid-liquid interface respectively. θ is the contact angle, which is influenced by the roughness of the material surface in theory. It is also can see that the smaller contact angle leads to great liquid content of the fiber.

Thus, in each simulation frame, we calculate the liquid absorption/ desorption rate of the contact area on the fiber-liquid interface and set as the maximum liquid absorption/desorption of the fiber segment. Meanwhile we figure out the saturated liquid content of the fiber according to regain property of the fiber. When the particle has collision with the fiber segment surface, if the fiber segment is under saturated liquid content, the particle will be absorbed, and if the fiber segment has reached the maximum liquid content, the particle will be bounced off or roll on the surface according to its momentum. On the other hand, if the maximum liquid absorption/desorption of the fiber segment is over the saturated liquid content, the liquid will be desorbed. In this case, new particles are generated with an initial speed according to the liquid concentration difference between the

inner and outer of the fiber segment and located on the fiber surface where there are sparse particles.

5.3. Liquid diffusion

During the liquid wetting process, liquid will diffuse from the location with high concentration to the location with low concentration. Due to the anisotropic structure of porous textile, the liquid diffusion across the textile is also anisotropic. When the fiber is wetted, the liquid will diffuse within the fiber and diffuse to the intersected fiber through contact area. Meanwhile, the liquid will also diffuse in the pores of textile caused by the capillary effect. Thus, we simulate the liquid diffusion by considering the ways of intersected fibers diffusion, inner fiber diffusion and capillary diffusion.

Consider the anisotropic diffusion and the influence of non-linear fiber liquid absorption/desorption on the concentration, the liquid diffusion across the porous textile is not a steady process, thus we describe this process based on the second Fick' law:

$$\frac{\partial C}{\partial t} = \frac{\partial}{\partial x}\left(D\frac{\partial C}{\partial x}\right) \tag{9}$$

where C is the liquid concentration, x is the diffusion distance, and D is the diffusion coefficient of liquid, which is dynamically determined by the concentration gradient in a differential unit. $D\frac{\partial C}{\partial x}$ is the diffusion flux. D will have different calculation methods in different ways of intersected fibers diffusion, inner fiber diffusion and capillary diffusion.

1) Inner fiber diffusion

When the fiber absorbs a certain amount of liquid, the most common way of liquid diffusion is in the inner fiber. When there is concentration gradient, the liquid will diffuse along the direction of gradient. The diffusion rate of the liquid is dependent on the diffusion coefficient, which can be determined by kunzel's diffusion coefficient as in Eqs.8. In the geometric construction, the fiber is consisted of fiber segments, while this construction will not influence the liquid diffusion between connected fiber segments. The diffusion between the interfaces of the connected fiber segment is smooth.

2) Intersected fibers diffusion

Since the porous textile is made up by intersected fibers in the weft and warp directions, the weft fibers and warp fibers are touched together on the intersection points. When the liquid diffuses in the fiber material due to the

concentration gradient, the liquid will also possibly diffuse to the intersected fibers through the intersection points. Provided with that the fiber is made up by fiber segments, the liquid diffusion occurs between intersected fibers when existing concentration gradient between them. Theoretically, the diffusion rate between intersected fiber segments should be the same with that of inner fiber segment, since they contact each other closely in the intersection. However, in practice, there is possible to have little air in the intersection which will influence the liquid transfer rate. Thus, we concern this obstruction by an influence coefficient on the liquid diffusion coefficient of inner fiber as ηD.

3) Capillary diffusion

In the porous textile, the intersected fibers form pores between the fibers, which cause capillary action due to surface tension and adhesive driving forces. The liquid will be diffused toward dry regain in the pores. Compared with the fiber liquid sorption, capillary diffusion (also called capillary penetration) is faster and is the main means of liquid diffusion cross the porous textile. The complex mechanism of the capillary effect is generally described by the diffusion coefficient.

We adopted the formulation of apparent diffusion coefficient in thin capillaries [1] to calculate the diffusion coefficient for capillary diffusion :

$$D = D^* + \frac{RU}{48D} \tag{10}$$

where $D^*$is the coefficient of molecular diffusion, U is the mean velocity, R is the radius of the pores, which is related to the porosity of the textiles, and we can calculate R by assuming the pore is a thin tube:

$$R = \sqrt{\frac{\varepsilon_{textile} V_{textile}}{2\pi r_{fiber}(n_{segment} - 1)(n_{fiber} - 1)}} \tag{11}$$

where $V_{textile}$is the volume of the textile, $n_{segment}$ is the number of segments of a fiber, $n_{fiber}$is the number of fibers in the weft direction.

In the geometric structure, a capillary pore is surrounded by 8 fiber segments. When the liquid is diffused by capillary effect and wets the surrounded fiber segments, liquid absorption/desorption by the fiber segments happens accordingly.

6. Simulation implementation

In the SPH-based fluid simulation, our implementation regards the particles as two types according to their locations, namely, the particles in the inner fluid and the particles on the boundary of the fluid. This distinction can be finished by the gradient of area density of the fluid, where if the gradient is close to zero the particles is in the inner fluid (here we set a threshold for the judgement), otherwise the particles is on the boundary. The inner particles will be exerted by the forces of pressure, viscosity and the gravity, thus their acceleration is the sum of the acceleration driven by these three forces. For the boundary particles, we further distinguish them into two situations. One is the particles near the liquid-vapor interface, where the particles are not only exerted by those three forces mentioned above, but also influenced by the force of surface tension. The force of surface tension will drive the boundary particles moving to the inner of the fluid. The other is the particles near the liquid-solid interface, where they will be additionally affected by the surface friction with the solid surface except for the pressure, viscosity, gravity and surface tension.

The algorithm is also capable to simulate the multi-drop of liquid wetting. In this framework, every drop of liquid is an independent particle system, adding a new drop means the merge with the existing particle system. That changes the previous space grids and the fluid boundary. Meanwhile, the doubled amount of particles will lead to possible dramatic change of area density and interior pressure, which may cause unpredictable results since the SPH system is very sensitive to the amount of particles. To solve this problem, we increase the time step between dripping two drops to avoid the suddenly crowded particles.

After the simulation, an important job is to visualize the liquid content of the textile during the wetting process. Since the fiber liquid absorption/desorption is calculated by the unit of fiber segments, the visualization of liquid content of the fiber is also realized segment by segment. We setup a color bar containing 11 colors to map the range of liquid content from zero to saturated liquid content of the fiber. The colors' value and transparency are evenly distributed with 10 levels in the blue belt to represent the ratio of current liquid concentration to saturated liquid concentration of the fiber segment (as shown in Fig.6), for instance, when the current liquid content of a fiber segment reaches saturation, it will be visualized with a blue and non-transparent color. And the case of the ratio with zero value is just mapped as white color without transparency. The visualization with

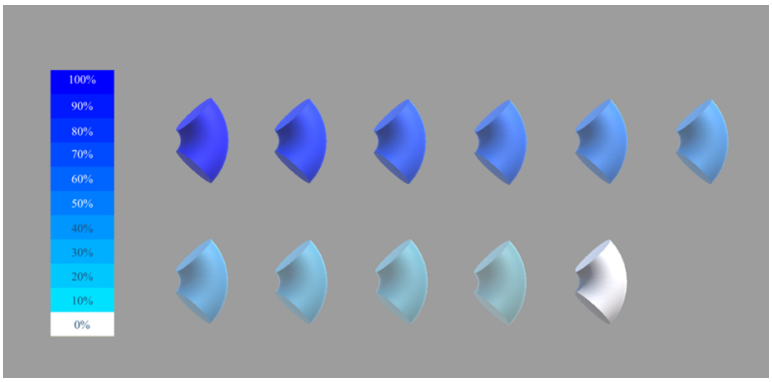

Figure 6: Color bar mapping the liquid concentration of the fiber segment.

11 levels of color difference is delicate to represent the dynamic change of liquid content of the fiber during wetting process.

7. Simulation results

All the simulation experiments are computed on C++ and shown with unity3D with hardware configuration of 3.5 GHz Intel Xeon E5-1620 v3 CPU and an NVIDIA Quadro K2200 4GB GPU. To achieve more accurate results, we set the time step between frames as 0.005s. We simulate the cases of textile with different contact angles, textile with different fiber materials and diffusion with multi-water drops. Table 1 and Table 2 show the parameters of the fibers in textiles construction and the parameters of particles in fluid simulation.

Table 1: The parameters of the fibers in textiles construction

Fiber radius(cm)	Fiber length/cm	Fiber number	Porosity
0.02	0.1	7200	0.98

7.1. Different fiber materials

In nature, different fiber materials have different hygroscopicity (also described as fiber regain), which also demonstrates that they have different liquid absorption coefficient (A_w) and saturated liquid volume (c_s) to influence the fiber liquid absorption/desorption. Thus, we can simulate and

Table 2: The parameters of particles in fluid simulation

Fluid density/ g/cm^3	Particle mass/g	Viscosity coefficient	Surface tension coefficient	Total particles
1.0	0.000205	0.2	0.001	8000

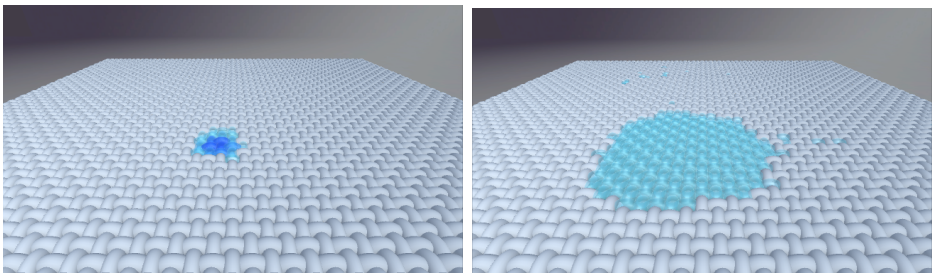

(a) Hydrophobic polyester (b) Hydrophilic wool

Figure 7: Simulation results of textiles consisted by hydrophobic polyester and hydrophilic wool fibers.

visualize the performance of different fiber materials in liquid wetting. Here we choose two different textiles consisted by hydrophobic polyester and hydrophilic wool to perform the simulation respectively. Fig.7 shows the simulation results. It can be seen that different fiber regains of polyester and wool lead to different performance in liquid diffusion. The lower fiber regain cause smaller kunzel diffusion coefficient, which lead to lower liquid absorption on the fiber and lower liquid diffusion through the fiber. On the other hand, higher fiber regain means higher saturated concentration, which enables the fiber to have higher liquid content. Thus we can see the wool textile has better performance of liquid diffusion than that of the polyester.

7.2. Multi-drops wetting simulation

The experiments in above are to investigate the influence of different properties of materials and are simulated with a single liquid drop. In order to visualize the continuous wetting process, we simulate the multi-drops wetting across a porous textile consisted by the wool fiber as in above. Fig.8 shows the continuous wetting process by three drops of liquid. The multi-drop liquid wetting process shows more details about liquid concentration

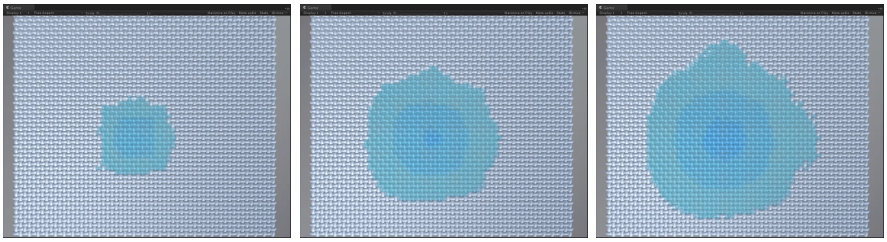

(a) One drop (b) Two drops (c) Three drops

Figure 8: Multidrop liquid wetting of porous anisotropic textiles.

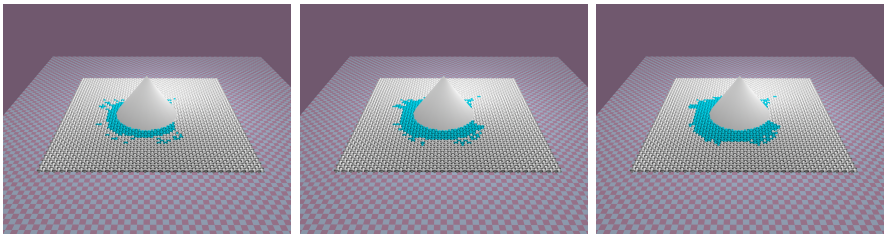

(a) One drop (b) Two drops (c) Three drops

Figure 9: Multidrop liquid wetting of porous anisotropic textiles along a cone.

difference in different areas during the diffusion process. With the more drops of liquid, the diffusion area is increasing through fiber absorption/desorption and liquid diffusion. Furthermore, we also simulate multi-drop liquid diffusing along a cone to wet the porous textile. As shown in Fig.9, the liquid continuously diffuse across the textile around the bottom the cone when the liquid drips on the top of the cone drop by drop.

8. Conclusion and future work

In this paper, we have presented a SPH-based simulation framework of liquid wetting across the porous textiles. Different from previous work, we realized the simulation on the consideration of real anisotropic inner structure of porous textile, which allows to really reflect the difference of textiles with different properties on liquid wetting. The surface tension and contact angle have been detail concerned in the simulation of fluid, and the liquid wetting process is described by the second Fick's law, which is capable to

model the non-steady fluid flow. The simulation framework can simulate the anisotropic liquid diffusion across the textile with the dripping of single or multiple drops of liquid. The simulation results investigate the influence of different properties of the textile material and the anisotropic wetting cross porous textiles by multi-drop liquid, which demonstrates the capability of our framework in achieving realistic simulation results. The directions of future work include: 1) improve the simulation and visualization to be synchronous, in the current work the visualization is performed after the simulation is finished, which can not provide a real-time observation of the liquid diffusion when changing the input; 2) allow the fiber segment to have shape change, such as inflation during diffusion to achieve more realistic simulation, which will involve more complex physical mechanisms.

References

[1] M. S. Bello, R. Rezzonico, and P. G. Righetti, *Use of Taylor-Aris dispersion for measurement of a solute diffusion coefficient in thin capillaries*, Science **266** (1994), no. 5186, 773–773.

[2] G. Bianchi, B. Solenthaler, G. Székely, and M. Harders, *Simultaneous topology and stiffness identification for mass-spring models based on fem reference deformations*, Medical Image Computing and Computer-Assisted Intervention–MICCAI 2004 (2004), 293–301.

[3] B. Bickel, M. Bächer, M. A. Otaduy, H. R. Lee, H. Pfister, M. Gross, and W. Matusik, *Design and fabrication of materials with desired deformation behavior*, in: ACM Transactions on Graphics (TOG), Vol. 29, 63, ACM (2010).

[4] D. E. Breen, D. H. House, and P. H. Getto, *A physically-based particle model of woven cloth*, The Visual Computer **8** (1992), no. 5, 264–277.

[5] D. E. Breen, D. H. House, and M. J. Wozny, *A particle-based model for simulating the draping behavior of woven cloth*, Textile Research Journal **64** (1994), no. 11, 663–685.

[6] M. Carlson, P. J. Mucha, and G. Turk, *Rigid fluid: animating the interplay between rigid bodies and fluid*, ACM Transactions on Graphics (TOG) **23** (2004), no. 3, 377–384.

[7] N. S.-H. Chu and C.-L. Tai, *MoXi: Real-time ink dispersion in absorbent paper*, ACM Trans. Graph. **24** (2005), no. 3, 504–511.

[8] G. Cirio, J. Lopez-Moreno, D. Miraut, and M. A. Otaduy, *Yarn-level simulation of woven cloth*, ACM Transactions on Graphics (TOG) **33** (2014), no. 6, 207.

[9] C. J. Curtis, S. E. Anderson, J. E. Seims, K. W. Fleischer, and D. H. Salesin, *Computer-generated Watercolor*, in: Proceedings of the 24th Annual Conference on Computer Graphics and Interactive Techniques, SIGGRAPH '97, 421–430, ACM Press/Addison-Wesley Publishing Co. (1997), ISBN 0-89791-896-7.

[10] B. Eberhardt, A. Weber, and W. Strasser, *A fast, flexible, particle-system model for cloth draping*, IEEE Computer Graphics and Applications **16** (1996), no. 5, 52–59.

[11] J. Gregson, M. Krimerman, M. B. Hullin, and W. Heidrich, *Stochastic tomography and its applications in 3D imaging of mixing fluids*, ACM Trans. Graph. **31** (2012), no. 4, 52–1.

[12] E. Guendelman, A. Selle, F. Losasso, and R. Fedkiw, *Coupling water and smoke to thin deformable and rigid shells*, ACM Transactions on Graphics (TOG) **24** (2005), no. 3, 973–981.

[13] M. Huber, S. Pabst, and W. Straßer, *Wet cloth simulation*, in: ACM SIGGRAPH 2011 Posters, 10, ACM (2011).

[14] H. M. Künzel, Verfahren zur ein-und zweidimensionalen Berechnung des gekoppolten Wärme-und Feuchtentransports in Bauteilen mit einfachen Kennwerten, Lehrstuhl Konstructive Bauphysik (1994).

[15] T. Lenaerts, B. Adams, and P. Dutré, *Porous flow in particle-based fluid simulations*, ACM Transactions on Graphics (TOG) **27** (2008), no. 3, 49.

[16] Y. Li and Z. Luo, *Physical mechanisms of moisture diffusion into hygroscopic fabrics during humidity transients*, Journal of the textile Institute **91** (2000), no. 2, 302–316.

[17] O. Mercier, C. Beauchemin, N. Thuerey, T. Kim, and D. Nowrouzezahrai, *Surface turbulence for particle-based liquid simulations*, ACM Transactions on Graphics (TOG) **34** (2015), no. 6, 202.

[18] Y. Morimoto, M. Tanaka, R. Tsuruno, and K. Tomimatsu, *Visualization of Dyeing based on Diffusion and Adsorption Theories*, in: Computer Graphics and Applications, 2007. PG '07. 15th Pacific Conference on, 57–64 (2007).

[19] J. P. Morris, *Simulating surface tension with smoothed particle hydrodynamics*, International journal for numerical methods in fluids **33** (2000), no. 3, 333–353.

[20] M. Müller, D. Charypar, and M. Gross, *Particle-based fluid simulation for interactive applications*, in: Proceedings of the 2003 ACM SIGGRAPH/Eurographics symposium on Computer animation, 154–159, Eurographics Association (2003).

[21] S. Patkar and P. Chaudhuri, *Wetting of porous solids*, IEEE transactions on visualization and computer graphics **19** (2013), no. 9, 1592–1604.

[22] X. Shi and S. Xiao, *Fluid absorption and diffusion in and between porous materials*, in: Proceedings of the 14th ACM SIGGRAPH International Conference on Virtual Reality Continuum and its Applications in Industry, 23–26, ACM (2015).

[23] P. Volino, N. Magnenat-Thalmann, and F. Faure, *A simple approach to nonlinear tensile stiffness for accurate cloth simulation*, ACM Transactions on Graphics **28** (2009), no. 4, Article–No.

[24] H. Wang, F. Hecht, R. Ramamoorthi, and J. F. O'Brien, *Example-based wrinkle synthesis for clothing animation*, ACM Transactions on Graphics (TOG) **29** (2010), no. 4, 107.

[25] X. Wang and V. Devarajan, *1D and 2D structured mass-spring models with preload*, The Visual Computer **21** (2005), no. 7, 429–448.

[26] X. Yan, Y.-T. Jiang, C.-F. Li, R. R. Martin, and S.-M. Hu, *Multiphase SPH simulation for interactive fluids and solids*, ACM Transactions on Graphics (TOG) **35** (2016), no. 4.

[27] S. Zhao, F. Luan, and K. Bala, *Fitting procedural yarn models for realistic cloth rendering*, ACM Transactions on Graphics (TOG) **35** (2016), no. 4, 51.

School of Computer Science and Engineering
South China University of Technology
Guangzhou, 510006, China
E-mail address: ahmao@scut.edu.cn

School of Computer Science and Engineering
South China University of Technology
Guangzhou, 510006, China
E-mail address: mingle@scut.edu.cn

Department of Computer Science and Technology
Tsinghua University
Beijing, 100084, China
E-mail address: liuyongjin@tsinghua.edu.cn

Department of Computer Science and Engineering
The Ohio State University
Columbus, OH 43210-1277, USA
E-mail address: whmin@cse.ohio-state.edu

School of Computer Science and Engineering
South China University of Technology
Guangzhou, 510006, China
E-mail address: ligq@scut.edu.cn